J Appl Electrochem
DOI 10.1007/s10800-017-1116-8

RESEARCH ARTICLE

Application of a nanostructured, tri-layer TiO_2 photoanode for efficiency enhancement in quasi-solid electrolyte-based dye-sensitized solar cells

M. A. K. L. Dissanayake[1,2] · H. N. M. Sarangika[1,2,3] · G. K. R. Senadeera[1,4] · H. K. D. W. M. N. R. Divarathna[1] · E. M. P. C. Ekanayake[1]

Received: 12 May 2017 / Accepted: 5 September 2017

Abstract A nanostructured, tri-layer TiO_2 photoanode consisting of a rice grain-shaped (RG), electrospun TiO_2 nanofiber layer (NF) sandwiched between two TiO_2 nanoparticle (NP) layers has been successfully used for the efficiency enhancement in quasi-solid-state electrolyte-based dye-sensitized solar cells (DSSCs). A polyethylene oxide-based quasi-solid-state or gel electrolyte with binary iodide salts with optimized composition was employed as the electrolyte. The solar cell parameters of this DSSC were compared with DSSCs fabricated using conventional NP TiO_2 photoanode. While the DSSCs fabricated with conventional NP photoanode showed an average efficiency of 5.76% with J_{sc} of 12.12 mA cm^{-2} and V_{oc} of 718.7 mV, the DSSCs fabricated with three-layer composite TiO_2 nanostructured photoanode (TiO_2 NP/RG/NP) showed an enhanced efficiency of 6.90% with J_{sc} of 16.93 mA cm^{-2} and V_{oc} of 672.3 mV. This shows that the three-layered composite photoanode with "rice grain-shaped" nanostructure is much superior to single-layered TiO_2 nanoparticle photoanode prepared by conventional method and evidently contributes to the efficiency enhancement by enhanced light harvesting by scattering. Post-treatment of the three-layer photoanode with $TiCl_4$ further enhanced the efficiency up to an impressive 7.30% which is among the highest for a quasi-solid-state DSSC.

✉ M. A. K. L. Dissanayake
makldis@yahoo.com

[1] National Institute of Fundamental Studies, Hantana Road, Kandy, Sri Lanka

[2] Postgraduate Institute of Science, University of Peradeniya, Peradeniya, Sri Lanka

[3] Department of Physical Sciences and Technology, Sabaragamuwa University of Sri Lanka, Belihul Oya, Sri Lanka

[4] Department of Physics, The Open University of Sri Lanka, Nawala, Nugegoda, Sri Lanka

Published online: 13 September 2017

Graphical abstract

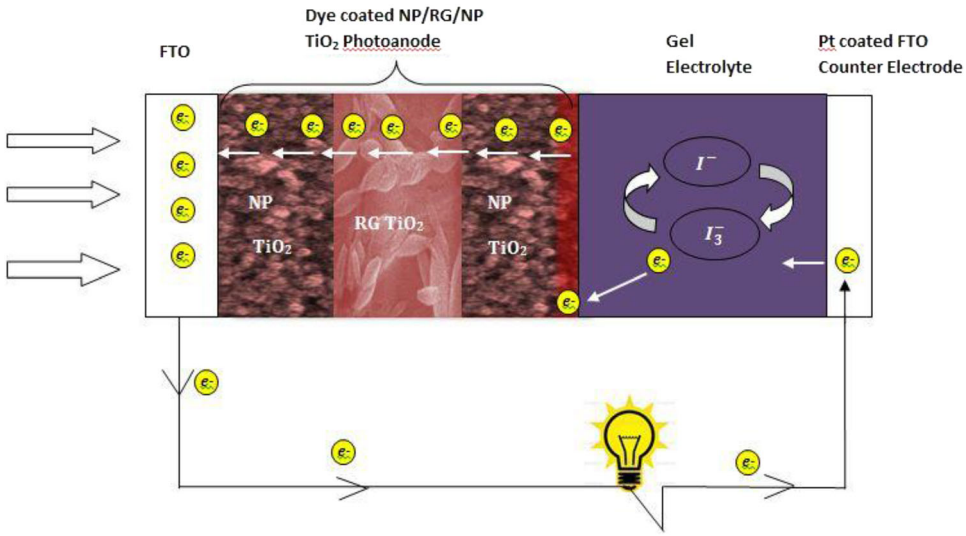

Keywords TiO_2 tri-layer photoanode · Electrospun TiO_2 nanofibers · Quasi-solid-state electrolyte · Dye solar cells · Efficiency enhancement

1 Introduction

After its invention by Gratzel [1], dye-sensitized solar cells (DSSCs) have emerged as an important and promising technology in photovoltaic field owing to their simple structure, transparency, design flexibility, low production cost, and a diverse range of possible applications. At present, major improvements in DSSCs have been realized by developing high-performance nanoporous TiO_2 thin film electrodes that have large surface area capable of adsorbing a large amount of photosensitizing dye enabling enhanced light harvesting. DSSCs using Ruthenium complex dyes, liquid electrolytes, and Platinum counter electrode have demonstrated reproducible conversion efficiencies of more than 11% under the illumination of 100 mW cm^{-2}. However, for their commercial applications, further improvements in the efficiency and stability of DSSCs are needed.

There are four main areas of research needed in order to enhance the overall performance of DSSCs. They can be categorized as development of (i) TiO_2 photoanode by nanostructural modifications, (ii) new electrolytes, (iii) new and low cost counter electrode, and (iv) new sensitizers. Among the work focused on developing counter electrodes, DSSCs with a new type of counter electrode (CE), composed of hydrophilic carbon (HC) particle and TiO_2 colloid (HC/TiO_2) showing impressive efficiencies close to those using Pt counter electrodes, have been reported [2]. Some important work on the development of photoanodes in DSSCs can be found in the recent literature [3–7]. A review paper by Ye et al. discusses advances in DSSCs focusing on photoanodes, sensitizers, electrolytes, and counter electrodes [3]. A novel photoanode structure modified by porous flower-like CeO_2 microspheres as a scattering layer with a thin TiO_2 film deposited by atomic layer deposition (ALD) has achieved a significantly enhanced DSSC performance [4]. In a recent review article, the progress in the development of novel photoanodes for DSSCs covering the Effect of semiconductor material (e.g., TiO_2, ZnO, SnO_2, N_2O_5, and nano carbon), preparation, morphology, and structure (e.g., nanoparticles, nanorods, nanofibers, nanotubes, fiber/particle composites, and hierarchical structure) has been discussed [5]. Fan et al. have summarized the major progress in advanced nano/micromaterials to improve the photoanodes and enhance the energy conversion efficiencies of DSSCs [6]. Canever et al. have reported a protocol for fabricating a fiber-based photoanode for dye-sensitized solar cells, consisting of a light-scattering layer made of electrospun titanium dioxide NF on top of a blocking layer made of commercially available titanium dioxide NPs [7]. This, however, is a by-layer TiO_2 nanostructure, and therefore different from the present report where we have demonstrated a tri-layer photoanode consisting of rice grain-shaped (RG) structures TiO_2 NP/RG/NP.

Out of the novel methods for improving the photoanodes, nanostructural modification of TiO_2 electrode is expected to have a profound influence on the overall solar cell performance. In this context, photoanode materials with various morphologies such as nanoparticle, ordered meso-structured materials, and one-dimensional-structured materials (nanorods, nanowires, and nanotubes) have been widely studied and reported [8, 9]. In most of these cases, nanostructured TiO_2 material has been prepared by using

both dry and wet processes. In the past decade, several methods such as sol–gel, hydrothermal processes, electrochemical anodization, electrospinning, electrospray, electrodeposition, directional chemical oxidation, chemical vapor deposition, and laser pyrolysis have been developed to control the size, morphology, and uniformity of the TiO_2 nanostructure [10].

Among various methods mentioned above, electrospinning is a simple and versatile nanofabrication technique. It can prepare several continuous 1-D nanofibers of polymers, ceramics, composites, and metals with controllable diameter ranging from few nanometers to several micrometers. The first discovery on electrospun TiO_2 nanofiber was reported in 2003, and subsequently many studies have been performed using electrospun TiO_2 nanofibers in photovoltaic devices [11, 12]. Fabrication of plasmonic AgBr/Ag nanoparticle-sensitized TiO_2 nanotube arrays and their enhanced photo-conversion and photoelectrocatalytic properties have been discussed by Wnag et al. [13].

However, as compared to TiO_2 nanofibers, nanoparticle TiO_2 electrode has higher surface-to-volume ratio. Therefore, the photocurrent of the DSSCs based on TiO_2 nanofibers is generally expected to be lower than that of TiO_2 nanoparticle photoelectrode. Thicker TiO_2 nanofiber photoanode with large surface area can be used in order to enhance the photocurrent. However, when the thickness is increased over the electron diffusion length in the photoanode, recombination probability will increase sharply thereby reducing the photocurrent [14]. Therefore, many research efforts have been focused on introducing light scattering layers to enhance the light harvesting efficiency [15, 16]. Taking these factors into consideration and to improve the light harvesting, a novel type of TiO_2 Nanofiber/Nanoparticle composite photoanode has been designed and tested [15]. This type of bi-layer TiO_2 nanofiber photoanode prepared by using both small and large diameter TiO_2 nanofibers has enhanced the efficiency of DSSCs from 7.14 to 8.40%. As reported by Joshi et al. [16], the composite made from electrospun TiO_2 nanofibers and conventional TiO_2 nanoparticles has also noticeably improved the light harvesting in DSSCs. Jung et al. [17] reported that the maximum efficiency of the DSSCs fabricated with highly porous nanofibers produced by electrospinning is significantly higher than that of DSSCs made with nanoporous TiO_2 nanofibers.

TiO_2 nanofiber films with rice grain-shaped structure can be prepared by calcinations of the nanofibers made from the electrospinning method [12, 18–20]. It has been found that these TiO_2 nanostructures posses high surface area, high porosity, and excellent inter-grain connectivity. There are several advantages of using these rice grain-shaped nanostructures as light scattering layers in DSSCs. As compared with spherical nanoparticles used in conventional DSSCs, these nanostructures could shorten the electron transport pathways and reduce the electron recombination. Zhu et al. reported that the DSSCs made with rice grain-shaped TiO_2 nanofibers as scattering layer showed a 15.7% increase in the overall efficiency of solar cells compared to the efficiency of DSSCs made with TiO_2 nanofibers [19]. Therefore, photovoltaic and photocatalytic performance of the rice grain-shaped structures appears to be superior to DSSCs made with TiO_2 nanofibers. It has been shown that TiO_2 rice grain-shaped nanostructure is beneficial for improved light scattering and charge transport [19].

An innovative, TiO_2 NP/RG/NP three-layer composite photoanode has been fabricated and tested by us in solution electrolyte-based DSSCs which has shown impressive efficiency enhancement evidently due to improved light harvesting by scattering [21]. The present paper reports the use of a similar tri-layer composite TiO_2 photoanode for efficiency enhancement in a quasi-solid–state (gel) electrolyte-based DSSC. To the best of our knowledge, this is the first report of a DSSC fabricated with such a three-layer composite nanostructured TiO_2 photoanode, combined with a "gel polymer electrolyte" exhibiting impressive cell efficiencies due to improved light harvesting. These research findings strongly support the suggestion that the mechanism of efficiency enhancement by increased light absorption by scattering within the tri-layer photoanode nanostructure in dye-sensitized solar cells is applicable irrespective of the nature of the electrolyte. Further enhancement of efficiency has been achieved by $TiCl_4$ treatment of the composite photoanode.

2 Experimental

2.1 Materials preparation and device fabrication

Polyvinylacetate (PVA, Mw = 140,000), titanium (IV) isopropoxide (TiP), *N-N* dimethylformamide (DMF), Polyethylene oxide (PEO) (Mw $\sim 4 \times 10^5$), and tetrapropyl ammonium iodide ($Pr4N^+I^-$) with purity >98% were purchased from Aldrich. Propylene carbonate (PC), ethylene carbonate (EC), iodine chips (I_2), and potassium iodide (KI) were purchased from Fluka. Ruthenium (N719) dye and TiO_2 nanoparticle paste (Solaronix D) were purchased from Soloronix SA.

2.1.1 Preparation of three-layered composite photoanode using electrospun TiO_2 nanofibers

Three-layered TiO_2 photoanode comprising with TiO_2 NP/RG/NP is fabricated by following the same procedure as mentioned in our previous publication [21]. In order to

fabricate DSSCs with $TiCl_4$-treated photoanodes, three-layer composite photoanodes prepared as described earlier were treated with titanium tetrachloride ($TiCl_4$). This treatment was done by immersing the photoanode in a 40 mM aqueous $TiCl_4$ solution at room temperature for 24 h. The electrodes were then washed with distilled water and sintered at 450 °C for 45 min. In order to compare the solar cell performances of the device fabricated with this three-layered photoanode, DSSCs were also fabricated comprising only with NP photoanodes, with a similar thickness by the "doctor blade method." After preparing above three types of photoanodes, they were then dipped in ethanoic dye solutions containing 0.3 mM of N719 dye at room temperature and left for 72 h for dye adsorption.

The electrolyte used for the DSSCs was prepared according to the following method. The amounts of PEO (0.1 g), EC (0.3 g) and PC (0.3 g) were kept unchanged and the mass ratio of the two ionic salts $Pr_4N^+I^-$ and KI were varied while the total weight of two salts was maintained at 0.12 g. The weight of the iodine was taken by keeping the salt to iodine ratio as 1:10 (Table 1).

First appropriate amounts of $Pr_4N^+I^-$ and KI (Table 1) were added to 0.3 g of PC and 0.3 g of EC and the mixture was stirred for few minutes for complete dissolution of the salts. Then, 0.1 g of PEO was added to this solution mixture and it was subsequently heated up to 80 °C under continuous stirring until a homogeneous viscous gel is formed. Iodine chips were added to the mixture at room temperature which was stirred for another 2 h in order to obtain a homogeneous gel electrolyte. This procedure was repeated for the preparation of other samples with different salt compositions.

2.1.2 Electrode morphology

The morphology of the electrospun nanofiber photoanodes was observed by the scanning electron microscopy (SEM) after the sintering process. The film thickness was measured by using SEM images of the cross section of the composite TiO_2 structure.

2.2 Measurements and characterization

2.2.1 Ionic conductivity measurements

Ionic conductivity of electrolyte samples was determined using computer-controlled Metrohm Autolab (PGSTAT 128N) impedance analyzer in the frequency range 0.1 Hz–10 MHz. For these measurements, polymer electrolyte samples were sandwiched between two polished stainless steel (SS) electrodes with the configuration SS/electrolyte/SS and impedance measurements were taken from the room temperature up to 65 °C at 5 °C intervals. Conductivity values at each temperature were determined from the impedance measurements.

2.2.2 I–V characteristics of the DSSCs

I–V characteristics of the devices comprising with three different photoanodes: (a) Conventional TiO_2 nanoparticle (NP) photoanode, (b) TiO_2 Nanoparticle/rice grain-shaped TiO_2 nano-fiber structure/TiO_2 nanoparticle (NP/RG/NP) three-layer composite photoanode and (c) $TiCl_4$-treated NP/RG/NP three-layer composite photoanode were compared under the illumination of 100 mW cm^{-2} (AM 1.5) simulated sunlight using a homemade computer-controlled setup coupled to a Keithley 2000 multimeter and potentiostat/galvanostat HA-301. To fabricate a complete DSSC, above dye-loaded photoanodes were assembled with aforementioned polymeric gel electrolytes and platinum-coated FTO glasses as shown schematically in Fig. 1. Each resulting solar cell had an active area of 0.25 cm^2.

2.2.3 Electrochemical impedance spectroscopy (EIS) measurements

In order to investigate the electron transport properties in the DSSCs comprising with above three types of photoanodes, EIS measurements were performed on them using the Metrohm Autolab Potentiostat/Galvanostat PGSTAT 128N coupled to a FRA 32 M Frequency Response Analyzer covering the 2 Hz to 100 kHz frequency range with an AC voltage signal of 10 mV. The electron recombination life time of above DSSCs was

Table 1 Weight percentages of KI, $Pr4N^+I^-$, and I_2 used for the preparation of the gel polymer electrolyte

Sample	KI wt% w.r.t. Pr_4NI wt	PC/g	EC/g	PEO/g	Pr_4NI/g	KI/g	I_2/g
A	0	0.3	0.3	0.1	0.12	0.0	0.009
B	25	0.3	0.3	0.1	0.09	0.03	0.012
C	40	0.3	0.3	0.1	0.07	0.05	0.015
D	50	0.3	0.3	0.1	0.06	0.06	0.014
E	60	0.3	0.3	0.1	0.05	0.07	0.015
F	100	0.3	0.3	0.1	0.00	0.12	0.018

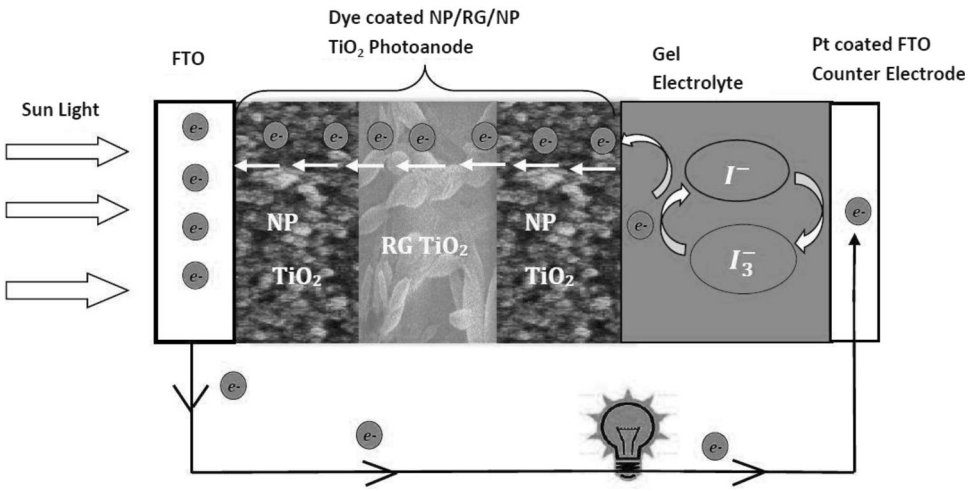

Fig. 1 Schematic diagram of the solar cell fabricated using rice grain-shaped TiO_2 nanostructure (not in scale)

estimated by using the impedance plots as well as plot of phase angle vs frequency (Bode phase plots). These measurements were carried out under the illumination of the same solar simulator under identical conditions. Dark *I–V* measurements were also taken for DSSCs made with these three types of photoanodes. The onset voltages under reverse bias characteristics were recorded in order to estimate the suppression of electron recombination. The external quantum efficiency (EQE) experiments were performed using a Bentham PVE300 unit and a TMC 300 optical monochromator equipped with a xenon arc lamp. A calibrated type DH photodetector was used as the reference.

3 Results and discussion

3.1 Characterization of the gel polymer electrolyte

Figure 2 shows the conductivity (on log scale) variation with the reciprocal of the absolute temperature for the gel polymer electrolyte samples prepared according to the compositions given in Table 1. The temperature dependence of the ln (σT) shows a linear behavior for all the measured compositions.

This linear behavior in the graphs suggests that the temperature dependence of the conductivity obeys the classical Arrhenius behavior given by the equation,

$$\sigma = \sigma_o \exp(-E_a/RT), \quad (1)$$

where σ is the ionic conductivity; σ_o is a constant; E_a is the activation energy; R is the gas constant, and T is the temperature in Kelvin. Room temperature (25 °C) conductivity values obtained for the compositions with 100% KI (0% $Pr4N^+I$) and 100% $Pr_4N^+I^-$ (0% KI) are 1.97×10^{-2} and 6.01×10^{-3} S cm^{-1}, respectively.

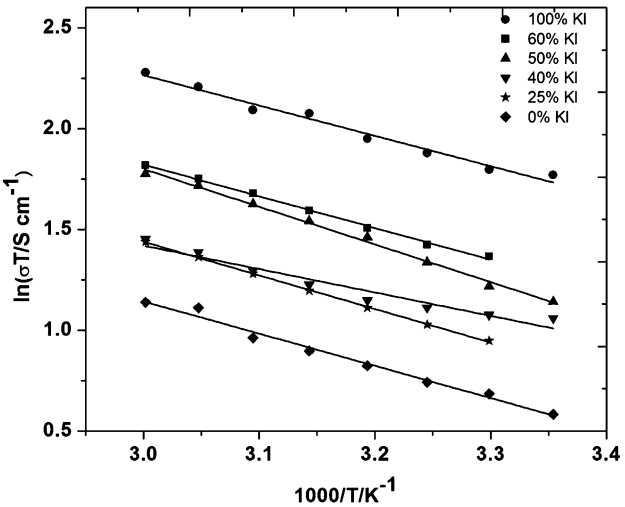

Fig. 2 The ln (σT) vs 1000/T graphs for different electrolyte compositions in the gel electrolyte system PEO:EC:PC: $Pr4N^+I + x$ wt% KI:I_2

The total ionic conductivity of the electrolyte is made up of individual conductivity contributions from K^+, Pr_4N^+, I^-, and I_3^- ions. It is clear from Fig. 2 that the conductivity values have gradually increased with increasing of KI concentration. Compared to the size of the Pr_4N^+ cation, K^+ cation is much smaller in size and therefore leads to a higher mobility. This could be the reason for increasing the total ionic conductivity values with increasing the KI concentration [22].

3.2 Morphology of the electrospun, rice grain-shaped TiO_2 nanostructure, TiO_2 nanoparticle layer, and the cross section of the tri-layer TiO_2 photoanode

Figure 3a shows the SEM image of electrospun TiO_2 nanofibers sintered at 450 °C for 1 hour in air. Figure 3b

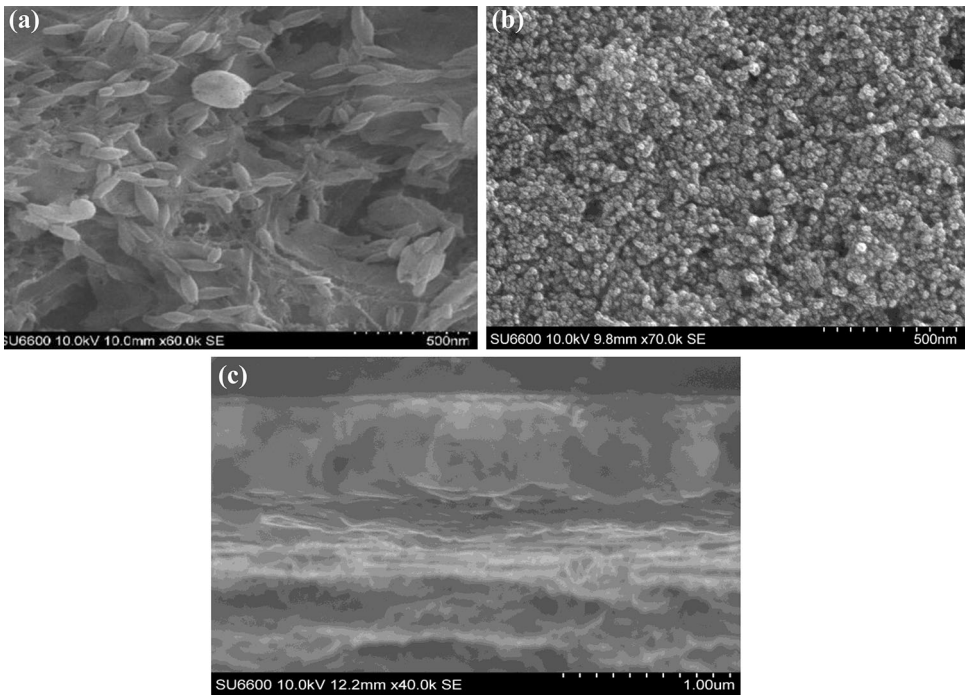

Fig. 3 **a** SEM image of the electrospun TiO_2 nanofibers after sintering at 450 °C showing the rice grain-shaped nanostructure. **b** SEM image of the TiO_2 nanoparticles after sintering at 450 °C. **c** Cross section SEM image of the TiO_2 NP/RG/NP three-layer composite photoanode. In the cross section image, from the top: Glass substrate/FTO layer/TiO_2 NP layer (3.0 μm)/TiO_2 NF(RG) layer (1.5 μm)/TiO_2 NP layer (1.5 μm). **c** is taken from Ref. [21]

shows the SEM image of the TiO_2 nanoparticle layer after sintering at 450 °C. Figure 3c shows the cross section SEM image of the TiO2 NP/RG/NP tri-layer photoanode. The resulting rice grain-shaped (RG) nanostructure can clearly be seen in the SEM image in Fig. 3a.

In the electrospinning method, there are several factors such as the applied voltage between the needle and the collector plate, tip to collector distance, flow rate, concentration, and viscosity of the electrolyte which can directly affect the morphology, porosity, and shape and the diameter of the electrospun nanofibers [23]. The electrospinning conditions we used in this study have resulted in the formation of these rice grain-shaped nanostructures after sintering the nanofibers.

According to the SEM analysis, the average dimensions of the rice grain-shaped nanostructures were 260 nm in length and 70 nm in width. Practically, it was difficult to obtain clear cross-sectional SEM images of the tri-layer photoanode structure. However, from cross section SEM images (Fig. 3c), the thicknesses of the three TiO_2 layers can be estimated as follows: First layer, on FTO, 3.0 μm; Middle layer of rice grain-shaped NF layer, 1.5 μm and the third layer (top layer), 1.5 μm [21]. The shape of a TiO_2 elongated grain-shaped nanostructure with two sharp ends appears to well match with the shape of a typical rice grain. Similar type of TiO_2 nanostructures has also been reported by Shengyuan et al. [12]. As it is observed by Hore et al., this elongated grain-shaped crystallite appears to be favorable for enhancing the light scattering ability inside the composite TiO_2 photoanode [24].

3.3 I–V characteristics of DSSC with mixed cation iodide salts

In order to see the combined effect of the three-layer (NP/RG/NP) composite TiO_2 photoanode and the mixed cation iodide salts containing gel electrolyte on the performance of the DSSCs, the cells were fabricated using configuration FTO/TiO_2/dye/electrolyte/Pt/FTO with gel electrolytes having different KI/Pr_4N^+I concentration ratios. Figure 4 shows the variation of current density (J_{sc}) vs voltage (V) of the DSSCs with three selected KI salt concentrations (for clarity) in the electrolyte.

Solar cell parameters for DSSCs fabricated with six different KI/Pr_4N^+I concentration ratios obtained from I–V curves are shown in Table 2. Corresponding variations of J_{sc} and efficiency as a function of KI% are shown in Fig. 5.

As shown in Table 2 and Fig. 5, the current density (J_{sc}) as well as the efficiency (η%) have increased with increasing KI concentration in the electrolyte up to 50 wt% KI, at the expense of the open-circuit voltage (V_{oc}). The maximum cell efficiency of 6.90% was obtained with a FF of 60.6% for the DSSC made with electrolyte (D) containing 50% KI and 50% $Pr_4N^+I^-$. The corresponding values for J_{sc} and V_{oc} were 16.93 mA cm^{-2} and 672.3 mV, respectively. The efficiency of the two DSSCs with end member electrolyte compositions (A and F) with 100% $Pr_4N^+I^-$ and 100% KI has exhibited current densities (J_{sc}) of 14.42 and 15.57 mA cm^{-2}, open-circuit voltages (V_{oc}) of 713.6 mV and 651.7 mV, fill factors (FF) of 55.7 and 60.24% and efficiencies (η%) of 5.70 and 6.11%,

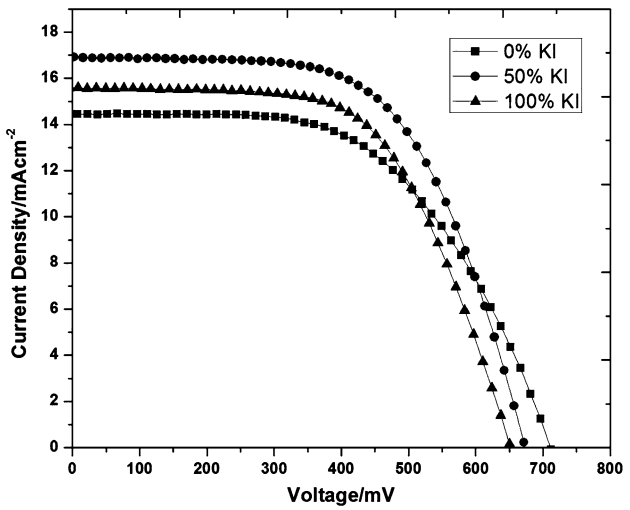

Fig. 4 Photocurrent–photovoltage (*I–V*) characteristics of solar cells with configuration FTO/TiO_2/dye/electrolyte/Pt/FTO fabricated with the three-layer composite TiO_2 photoanode (NP/RG/NP) for three different electrolyte compositions (KI/Pr_4N^+I concentration ratios): 0 wt% KI, 50 wt% KI, and 100 wt% KI

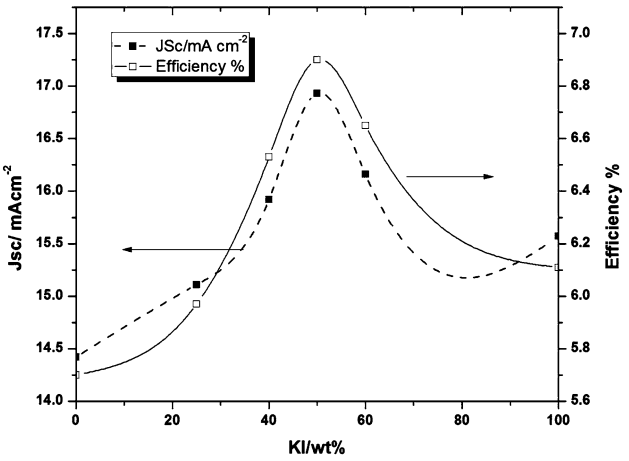

Fig. 5 Variation of the efficiency and the short circuit current density of DSSCs with respect to the KI wt% in the electrolyte with KI/Pr_4N^+I with three-layer TiO_2 photoanode, NP/RG/NP

respectively. It is interesting to note that, although the electrolyte with 100% KI composition has shown the highest overall ionic conductivity, the highest DSSC efficiency was shown by the electrolyte containing 50% of KI and 50% of Pr_4N^+ (Table 2). This suggests that it is the anionic (or iodide ion) conductivity of the electrolyte, which is important for a DSSC as it determines the short-circuit photocurrent density.

It is clear from this table and the figure that DSSCs with mixed cation iodide salts give the highest device performance. The efficiency enhancement due to cation adsorption in the TiO_2 photoanode in DSSCs with mixed cation iodide salts used both in gel- and liquid-type electrolytes have been studied in detail by our group since 2012 and subsequently by few other groups [25–27]. The increase in current density with increasing KI concentration can be attributed to the enhancement of the current density due to the adsorption of small size (K^+) cations by the TiO_2 electrode. Adsorption of small cations such as Li^+ and K^+ by the TiO_2 photoanode causes a positive shift in the TiO_2 conduction band as confirmed in our previous studies, facilitating the electron transfer dynamics and charge injection rate at the electrode/electrolyte interface and hence increasing the current density (J_{sc}) at the expense of the V_{oc}. Iodide salts with bulky cations such as Pr_4N^+ on the other hand contribute to a smaller conduction band shift and therefore a higher V_{oc}. Thus, the use of a binary mixture of two iodide salts with small and large cations can maximize the current density and efficiency of the DSSCs at an intermediate relative cation concentration [22].

As shown in Fig. 5, the efficiency variation with KI salt concentration follows the same trend as the photocurrent density. Both J_{sc} and efficiency exhibit maxima at 50% wt KI concentration suggesting the optimized situation resulting from the two competing effects described above by the small-sized and large-sized cations in the electrolyte.

3.4 Effect of the three-layer NP/RG/NP composite TiO_2 photoanode on efficiency enhancement in DSSCs

Current–voltage characteristic curves of the DSSCs fabricated using above three different types of photoanodes, (a),

Table 2 Parameters for the solar cells with PEO:EC:PC: Pr4N$^+$I + *x* wt% KI:I_2 gel polymer electrolyte as a function of KI wt% and with three-layer TiO_2 photoanode, NP/NF(RG)/NP

DSSC	KI wt% (in the electrolyte)	J_{sc} (mA cm^{-2})	V_{oc} (mV)	*FF%*	*η%*
A	0	14.42	713.6	55.71	5.70
B	25	15.11	708.9	55.72	5.97
C	40	15.92	687.9	59.63	6.53
D	**50**	**16.93**	**672.3**	**60.62**	**6.90**
E	60	16.16	660.5	62.37	6.65
F	100	15.57	651.7	60.24	6.11

The bold fonts correspond to the solar cell with highest efficiency

(b), and (c) comprising with the gel electrolyte consisting of optimized composition of the binary mixture of iodide salts, are shown in Fig. 6. Table 3 summarizes the photovoltaic parameters obtained from the Fig. 6.

As shown in Table 3, the DSSC fabricated with the conventional NP photoanode showed an efficiency of 5.76%. Incorporation of rice grain-type nanostructured three-layered photoanode in the DSSC with the same electrolyte enhanced the efficiency of the device up to 6.90%. Moreover, the DSSCs fabricated with $TiCl_4$-treated three-layered photoanode showed an efficiency of 7.32% showing an impressive 27% enhancement in the overall efficiency compared to the DSSC fabricated with conventional TiO_2 NP photoanode.

Song et al. [28, 29] reported that DSSCs fabricated with TiO_2 nanofiber photoanode and gel electrolyte showed an energy conversion efficiency of 94.7% of that of liquid electrolyte-based DSSC confirming the effective penetration of viscous gel electrolyte through the TiO_2 nanofiber electrode due to the porous morphology of the nanofiber structure.

3.5 Enhanced light harvesting by scattering

The "rice grain like" nanostructure formed from the sintered TiO_2 nanofibers could affect the porosity, effective surface area, light scattering, and electron transport rate in the composite TiO_2 photoanode. As suggested by Zhu et al. in a similar study [19], the enhancement of the photocurrent density is quite likely due to the improved light harvesting by scattering by the TiO_2-elongated rice grain-shaped nanostructure in the composite photoanode. Joshi et al. [16] have reported a similar improvement in light harvesting due to light scattering by a composite photoanode consisting of a mixture of TiO_2 nanofibers and nanoparticles. In the present work also, the increase in J_{sc} is very likely due to the light scattering effect by the TiO_2 elongated rice grain-like nanostructure sandwiched between two TiO_2 nanoparticle layers in the composite three-layer photoanode. These elongated bead-like nanostructures, which are randomly distributed within the TiO_2 RG nanofiber layer in the composite photoanode, can scatter incident light effectively resulting in a substantial increase in light absorption by the dye molecules in the composite photoanode. Comparing with the different photoanode structures reported by several groups such as by Zhu et al. [19], Joshi et al. [16], and Tan et al. [30], the three-layered novel photoanode proposed in this study is capable of more efficient light trapping due to multiple scattering events within the NF layer resulting an enhanced photocurrent density.

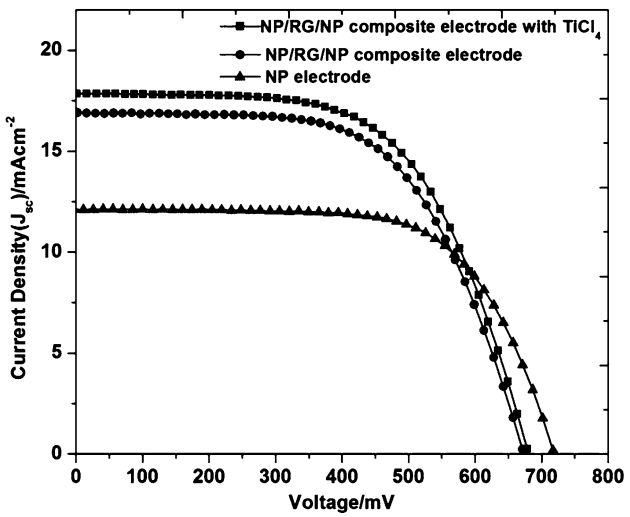

Fig. 6 Photocurrent–photovoltage (*I–V*) characteristics curves for solar cells with configuration FTO/TiO_2/dye/electrolyte/Pt/FTO fabricated with three different TiO_2 photoanodes, **a** NP, **b** NP/RG/NP, and **c** NP/RG/NP $TiCl_4$ treated. The optimized composition of the gel electrolyte used was PEO:EC:PC: 50% Pr_4N^+I + 50% KI:I_2

Table 3 Parameters for the solar cells fabricated with three different types of photoanodes with PEO:EC:PC: 50%Pr_4N^+I + 50%KI:I_2 mixed cation gel polymer electrolyte

	Type of photoanode		
	NP	NP/RG/NP	$TiCl_4$ treated NP/RG/NP
V_{oc} (mV)	718.7	672.3	678.8
J_{sc} (mA cm^{-2})	12.12	16.93	17.83
Fil factor (%)	66.07	60.62	60.51
Efficiency (%)	5.76	6.90	7.32

As it is evident from Fig. 6 and Table 3, the DSSC fabricated with $TiCl_4$-treated three-layer photoanode is capable of delivering 7.32% efficiency with higher photocurrent density than the other two types of DSSCs. Similar efficiency enhancement due to $TiCl_4$ treatment has been interpreted and reported by several groups [31–33]. The widely accepted explanation is that the $TiCl_4$ treatment increases the effective surface area of the TiO_2 photoanode by filling the gaps between nanoparticles/nanostructures in the TiO_2 film, resulting in an increase in dye loading and light harvesting. It is also supposed to facilitate the electron transfer by blocking the charge recombination at the interface between the conduction glass FTO and the I_3^- ions present in the I^-/I_3^- redox electrolyte. Both these factors would enhance the photocurrent density and the overall power conversion efficiency of the solar cells (Table 3; Fig. 5). The present work supports the argument that the post-$TiCl_4$ treatment works well even with sandwich-type photoanodes with a nanofiber layer in between.

3.6 Electrochemical impedance spectroscopic (EIS) analysis

Figure 7 shows the Nyquist plots of the electrochemical impedance spectra of cells fabricated with three different photoanodes (a), (b) and (c), under the illumination of 100 mW cm^{-2} (AM 1.5).

Nyquist plots of the electrochemical impedance spectra were taken in the frequency range from 1×10^{-2} to 1×10^{6} Hz. The Nyquist plot exhibits two semi-circles including a large semi-circle at low frequency and a small one at high frequency. The small semi-circle in the high frequency range can be assigned to the charge transfer resistance (R1ct) at the redox electrolyte/Pt counter electrode or TiO_2 interface. The large semi-circle in the low frequency region can be attributed to the transport of injected electrons within the TiO_2 film and the charge transfer across either the TiO_2/redox electrolyte interface or TiO_2/FTO interface [34]. The impedance parameters were extracted from the equivalent circuit model shown in the inset. The calculated values of the series resistance (R_s), the charge transfer resistance of the Pt/electrolyte interface ($R1_{ct}$), and the charge transfer resistance of TiO_2/electrolyte interface ($R2_{ct}$) for the three types of DSSCs fabricated with three different electrodes are summarized in Table 4. As it is evident from Table 4, DSSC fabricated with NP/RG/NP composite electrode shows lower $R1_{ct}$, $R2_{ct}$ and R_s resistances compared to those with the DSSC fabricated with conventional NP-TiO_2 photoanode. Further reduction of these resistance values can be seen with the DSSC fabricated with $TiCl_4$-treated photoanode.

From these results, it is clear that the $R2_{ct}$ value, which refers to charge transfer resistance of TiO_2/electrolyte interface, has gradually decreased by the modification of

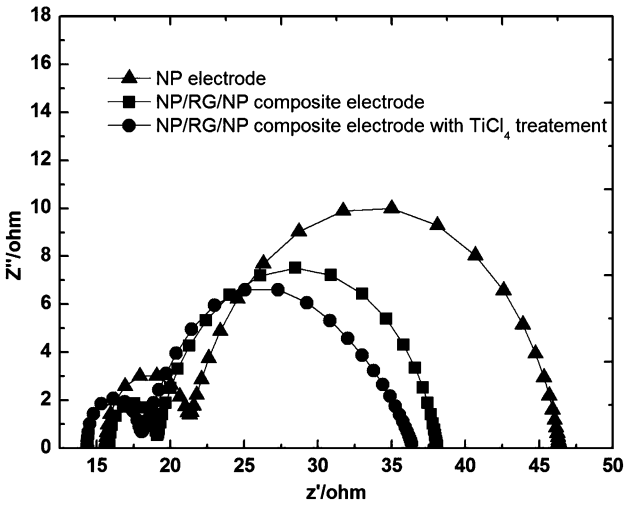

Fig. 7 Nyquist plots of the DSSCs with configuration FTO/TiO_2/dye/electrolyte/Pt/FTO fabricated with the three types of TiO_2 photoanodes **a** NP, **b** NP/RG/NP, and **c** NP/RG/NP $TiCl_4$ treated

TiO_2 photoanode with rice grain-shaped nanostructure and $TiCl_4$ treatment. The low value of $R2_{ct}$ facilitates more efficient electron transport at TiO_2/electrolyte interface [34] while increasing the number of injected electrons into the TiO_2 film and reducing the charge recombination rate. According to the studies of electron/charge transport in TiO_2 nanofibers, nanowires, and nanorods, the electrospun nanofibers and nanorods exhibit high electron diffusion [16]. Saji et al. have recently reported that 10% nanorods–nanoparticle composite matrix leads to reduced charge transport resistance [35]. Kim et al. reported that electron transport of TiO_2 nanofiber–nanoparticle composite electrode can be enhanced with $TiCl_4$ treatment [16]. Therefore, our findings with three-layered TiO_2 NP/RG//NP composite photoanode are in agreement with the reported results by the other groups.

As observed by the others, the reduction of the second semi-circle in the Nyquist plots with the $TiCl_4$ treatment is possibly due to an increase in the packing density and facilitate in the enhancement in the charge transport through TiO_2 electrode while reducing the rate of charge recombination [28]. These results are also consistent with the results obtained from the Bode phase plot of the three different cells. Therefore, with the EIS analysis, it can be confirmed that the charge recombination between injected electrons and the redox electrolyte is reduced in the DSSCs with NP/NF(RG)/NP composite electrode compared to the DSSC with conventional NP-TiO_2 photoanode.

Figure 8 shows the variations of phase angle vs frequency data (Bode plots) obtained from the impedance measurements on above three types of photoanodes. It can be observed that peak value of the characteristic frequency of three-layered NP/RG/NP TiO_2 photoanode is lower than the conventional type of TiO_2 NP photoanode and further reduction can be observed with the $TiCl_4$ treatment. This characteristic frequency is related to the inverse of the recombination life time (τ) in photoanode as defined by the following equation.

$$\tau = \frac{1}{\omega_{\min}} = \frac{1}{2\pi f_{\max}} \tag{2}$$

Table 5 summarizes the calculated data and it can be clearly observed that recombination lifetime for DSSCs fabricated with $TiCl_4$-treated NP/RG/NP has the highest value of 18.19 ms as compared to 16.99 ms for NP/RG/NP composite photoanode and 8.61 ms for conventional NP photoanode. Therefore, it is evident from the estimated values of charge transfer resistance and the recombination life time; the presence of nanostructured, rice grain-shaped TiO_2 thin layer increases the electron lifetime and makes the electron transfer more efficient. This means that the charge transfer resistance in TiO_2/electrolyte interface and electron recombination have decreased leading to a

Table 4 Series resistance (R_s), charge transfer resistance of the Pt/electrolyte interface ($R1_{ct}$), and charge transfer resistance of TiO_2/electrolyte interface ($R2_{ct}$) for the three types of DSSCs fabricated with three different TiO_2 photoanodes, (a) NP, (b) NP/NF(RG)/NP, and (c) NP/RG/NP $TiCl_4$ treated

Estimated resistance values	Type of photoanode used in DSSC		
	NP	NP/RG/NP	$TiCl_4$-treated NP/RG/NP
R_s/Ω	15.7	15.9	14.4
$R1_{ct}/\Omega$	5.47	3.13	3.49
$R2_{ct}/\Omega$	25.3	19.1	18.2

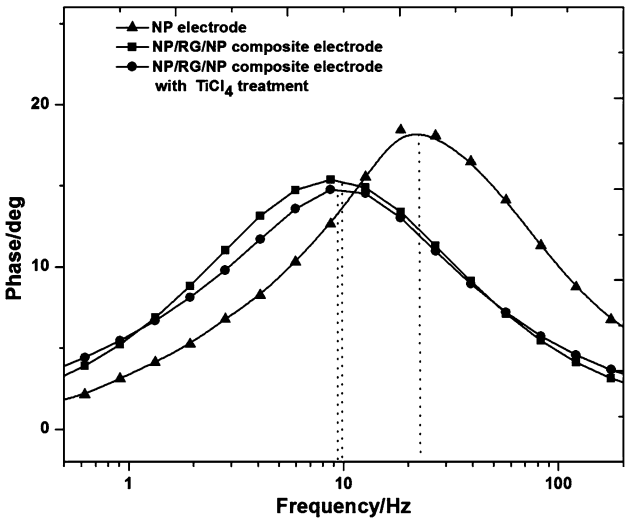

Fig. 8 Impedance data plotted as phase angle versus frequency (Bode plots) for the three DSSCs fabricated with three different TiO_2 photoanodes **a** NP, **b** NP/RG/NP, and **c** NP/RG/NP $TiCl_4$ treated

Table 5 Electron recombination life times extracted from the impedance spectra by fitting appropriate equivalent circuits

Type of photoanode used in DSSC	Efficiency of DSSC (%)	Frequency (Hz)	ι (ms)
NP-TiO_2 electrode	5.76	18.48	8.61
NP/NF(RG)/NP	6.90	9.37	16.99
$TiCl_4$-treated NP/RG/NP	7.32	8.75	18.19

positive influence on cell performance. These results are consistent with the current densities (J_{sc}) of the three DSSCs listed in Table 3. As expected, the highest J_{sc} of the DSSCs corresponds to the NP/RG/NP composite electrode with $TiCl_4$ treatment. Therefore, the three-layered NP/RG/NP composite TiO_2 photoanode has the longest electron life time which could effectively reduce the electron recombination and consequently enhance the cell efficiency [34].

4 Conclusion

This work shows that the efficiency enhancement by a three-layer composite TiO_2 photoanode consisting of TiO_2 NP/RG/NP where RG refers to "rice grain-shaped" electrospun nanofibers, and NP refers to nanoparticles, can be extended to DSSCs fabricated with PEO-based quasi-solid-state (gel) polymer electrolytes as well. An impressive enhancement in the efficiency has been achieved by replacing the conventional TiO_2 nanoparticle (NP) photoanode by the three-layer composite NP/RG/NP TiO_2 photoanode evidently due to the improved light harvesting by scattering by the three-layer TiO_2 photoanode nanostructure, reduction of charge transfer resistance, and the enhancement in the electron recombination life time. The mixed cation effect in the PEO-based polymeric gel electrolyte with binary cation iodide salt and post-$TiCl_4$ treatment have further improved the photovoltaic performance. The overall DSSC efficiency of 7.32% achieved in this work is among the highest for gel electrolyte-based DSSCs.

Acknowledgements HNMS wishes to acknowledge the National Institute of Fundamental Studies (NIFS) for providing research facilities and Sabaragamuwa University of Sri Lanka for granting study leave to complete this project successfully.

References

1. O' Regan B, Grätzel M (1991) A low-cost, high-efficiency solar cell based on dye-sensitized colloidal TiO_2 films. Nature 353:737–740
2. Kouhnavard M, Ludin NA, Ghaffari BV, Ikeda S, Sopian K, Miyake M (2016) Hydrophilic carbon/TiO_2 colloid composite: a potential counter electrode for dye-sensitized solar cells. J Appl Electrochem 46(2):259–266
3. Ye M, Wen X, Wang M, Iocozzia J, Zhang N, Lin C, Lin Z (2015) Recent advances in dye-sensitized solar cells: from photoanodes, sensitizers and electrolytes to counter electrodes. Mater Today 18(3):155–162
4. Song W, Gong Y, Tian J, Cao G, Zhao H, Sun C (2016) Novel photoanode for dye-sensitized solar cells with enhanced light-harvesting and electron-collection efficiency. ACS Appl Mater Interfaces 8(21):13418–13425
5. Liu X, Fang J, Liu Y, Lin T (2016) Progress in nanostructured photoanodes for dye-sensitized solar cells. Front Mater Sci 10(3):225–237
6. Fan K, Yu J, Ho W (2017) Improving photoanodes to obtain highly efficient dye-sensitized solar cells: a brief review. Mater Horiz 4:319–344
7. Canever N, Hughson F, Macdonald TJ, Nann T (2017) Electrospinning of photocatalytic electrodes for dye-sensitized solar cells. J Vis Exp 124:e55309. doi:10.3791/55309
8. Grätzel M (2003) Dye-sensitized solar cells. J Photochem Photobiol C 4:145–153
9. Senadeera GKR, Kobayashi S, Kitamura T, Wada YS, Yanagida S (2005) Versatile preparation method for mesoporous TiO_2 electrodes suitable for solid-state dye sensitized photocells. Bull Mater Sci 28(6):635–641

10. Lin Z, Wang J (2003) Polymer nanofibers assembled by electrospinning. Curr Opin Colloid Interface Sci 8:64–75
11. Frenot A, Chronakis IS (2003) Polymer nanofibers assembled by electrospinning. Curr Opin Colloid Interface Sci 8:64–75
12. Shengyuan Y, Peining Z, Nair AS, Ramakrishna S (2011) Rice grain-shaped TiO_2 mesostructures-synthesis, characterization and applications in dye-sensitized solar cells and photocatalysis. J Mater Chem 21:6541–6548
13. Wang Q, Qiao J, Jin R, Xu X, Shanmin Gao S (2015) Fabrication of plasmonic AgBr/Ag nanoparticles-sensitized TiO_2 nanotube arrays and their enhanced photo-conversion and photoelectrocatalytic properties. J Power Sources 277:480–485
14. Li J, Chen X, Ai N, Hao J, Chen Q, Strauf S, Shi Y (2011) Silver nanoparticle doped TiO_2 nanofiber dye sensitized solar cells. Chem Phys Lett 514:141–145
15. Yang L, Leung WWF (2011) Application of a bilayer TiO2 nanofiber photoanode for optimization of dye-sensitized solar cells. Adv Mater 23:4559–4562
16. Joshi P, Zhang L, Davoux D, Zhu Z, Galipeau D, Fong H, Qiao Q (2010) Composite of TiO_2 nanofibers and nanoparticles for dye-sensitized solar cells with significantly improved efficiency. Energy Environ Sci 3:1507–1510
17. Jung WH, Kwak NS, Hwang TS, Yi KB (2012) Preparation of highly porous TiO_2 nanofibers for dye-sensitized solar cells (DSSCs) by electro-spinning. Appl Surf Sci 261:343–352
18. Nair AS, Shengyuan Y, Peining Z, Ramakrishna S (2010) Rice grain-shaped TiO_2 mesostructures by electrospinning for dye-sensitized solar cells. Chem Commun 46:7421–7423
19. Zhu P, Nair AS, Yang S, Peng S, Ramakrishna S (2011) Which is a superior material for scattering layer in dye-sensitized solar cells—electrospun rice grain-or nanofiber-shaped TiO_2? J Mater Chem 21:12210–12212
20. Nair AS, Zhu P, Babu VJ, Yang S, Krishnamoorthy T, Murugan R, Peng S, Ramakrishna S (2012) TiO_2 derived by titanate route from electrospun nanostructures for high-performance dye-sensitized solar cells. Langmuir 28:6202–6206
21. Dissanayake MAKL, Divarathna HKDWMN, Dissanayake CB, Senadeera GKR, Ekanayake PMPC, Thotawattage CA (2016) An innovative TiO_2 nanoparticle/nanofiber/nanoparticle, three layer composite photoanode for efficiency enhancement in dye-sensitized solar cells. J Photochem Photobiol A 322–323:110–118
22. Dissanayake MAKL, Thotawatthage CA, Senadeera GKR, Bandara TMWJ, Jayasundera WJMJSR, Mellander B-E (2012) Efficiency enhancement by mixed cation effect in dye-sensitized solar cells with PAN based gel polymer electrolyte. J Photochem Photobiol A 246:29–35
23. Dissanayake MAKL, Divarathne HKDWMNR, Thotawatthage CA, Dissanayake CB, Senadeera GKR, Bandara BMR (2014) Dye-sensitized solar cells based on electrospun polyacrylonitrile (PAN) nanofiber membrane gel electrolyte. Electrochim Acta 130:76–81
24. Hore S, Nitz P, Vetter C, Prahl C, Niggemann M, Kern R (2005) Scattering spherical voids in nanocrystalline TiO_2- enhancement of efficiency in dye-sensitized solar cells. Chem Commun 15:2011–2013
25. Arof AK, Aziz MF, Noor MM, Careem MA, Bandara LRAK, Thotawatthage CA, Rupasinghe WNS, Dissanayake MAKL (2014) Efficiency enhancement by mixed cation effect in dye-sensitized solar cells with a PVdF based gel polymer electrolyte. Int J Hydrog Energy 39(6):2929–2935
26. Dissanayake MAKL, Thotawatthage CA, Senadeera GKR, Bandara TMWJ, Jayasundara WJMJSR, Mellander B-E (2013) Efficiency enhancement in dye sensitized solar cells based on PAN gel electrolyte with $Pr_4NI + MgI_2$ binary iodide salt mixture. J Appl Electrochem 43:891–901
27. Dissanayake MAKL, Jayathissa R, Seneviratne VA, Thotawatthage CA, Senadeera GKR, Mellander B-E (2014) Polymethylmethacrylate (PMMA) based quasi-solid electrolyte with binary iodide salt for efficiency enhancement in TiO_2 based dye sensitized solar cells. Solid State Ionics 265:85–91
28. Song MY, Kim DK, Jo SM, Kim DY (2005) Enhancement of the photocurrent generation in dye-sensitized solar cell based on electrospun TiO_2 electrode by surface treatment. Synth Met 155:635–638
29. Song MY, Kim DK, Ihn KJ, Jo SM, Kim DY (2005) New application of electrospun TiO 2 electrode to solid-state dye-sensitized solar cells. Synth Met 153:77–80
30. Tan B, Wu Y (2006) Dye-sensitized solar cells based on anatase TiO2 nanoparticle/nanowire composites. J Phys Chem B 110:15932–15938
31. Lee S-W, Ahn K-S, Zhu K, Neale NR, Frank AJ (2012) Effects of $TiCl_4$ treatment of nanoporous TiO_2 films on morphology, light harvesting, and charge-carrier dynamics in dye-sensitized solar cells. J Phys Chem C 116(40):21285–21290
32. Li J, Zhang H, Wang W, Qian Y, Zhenghui Li Z (2016) Improved performance of dye-sensitized solar cell based on TiO_2 photoanode with FTO glass and film both treated by $TiCl_4$. Physica B 500:48–52
33. Vesce L, Riccitelli R, Soscia G, Brown TM, Di Carlo A, Andrea RA (2010) Optimization of nanostructured titania photoanodes for dye-sensitized solar cells: study and experimentation of $TiCl_4$ treatment. J Non-Cryst Solids 356(37–40):1958–1961
34. Xu H, Tao X, Wang DT, Zheng YZ, Chen JF (2010) Enhanced efficiency in dye-sensitized solar cells based on TiO_2 nanocrystal/nanotube double-layered films. Electrochim Acta 55:2280–2285
35. Saji VS, Pyo M (2010) Dye sensitized solar cell of TiO_2 nanoparticle/nanorod composites prepared via low-temperature synthesis in oleic acid. Thin Solid Films 518:6542–6546